physica status solidi rrl
www.pss-rapid.com

Passivation of Germanium Surfaces by HF:H_2O_2 Aqueous Solution

Mariia Terletskaia, Joonas Isometsä, Mikko Miettinen, Pekka Laukkanen, Ville Vähänissi, and Hele Savin*

Promising intrinsic electronic properties, such as narrow bandgap and high charge carrier mobilities, make germanium (Ge) a good replacement for silicon in optoelectronic applications (e.g., photodetectors). However, successful fabrication of efficient Ge devices requires minimization of both reflectance and surface recombination losses. This work begins with an observation that metal-assisted chemical etching (MACE) of Ge surfaces, used for optics improvement, reduces surface recombination without application of any intentional passivation. We proceed with investigation of the effect of MACE solution components and their mixtures on Ge surface passivation. The results demonstrate that HF:H_2O_2 aqueous solution leads to efficient and stable passivation. The film formed in this solution secures surface recombination velocity (S_{eff}) of 14 cm s^{-1}. Morphological and chemical characterization of the structure reveals porous germanium (PGe) layer with some GeO_x included. Finally, we propose several hypotheses on a mechanism behind this passivation, among which are the presence of GeO_2 at the film-bulk Ge interface and appearance of a potential barrier due to the hetero-junction formation. The presented Ge passivation with PGe layer provides a simple and cost-efficient alternative to existing state-of-the-art passivation schemes.

1. Introduction

Germanium (Ge) is currently contemplated to be a promising replacement for silicon (Si) in many applications, especially in optoelectronics, what is dictated by its good intrinsic electronic properties. The narrow bandgap (≈0.66 eV) of Ge is beneficial for light harvesting, e.g., in multijunction solar cell or photodetector (especially in near-infrared region) applications,[1–3] while the high charge carrier mobilities ($\mu_h \leq 1900\ cm^2 V^{-1} s^{-1}$, $\mu_e \leq 3900\ cm^2 V^{-1} s^{-1}$) allow greater switching speeds in complementary metal–oxide–semiconductor (CMOS) transistors.[4–6] Furthermore, the good compatibility of Ge with Si allows simple integration of Ge into Si-based electronics. This, in turn, enables technologies build on Ge-on-Si structures and SiGe alloys.[7–9]

Notwithstanding the merits of Ge in terms of electronic properties and light absorption facilitated by the narrow bandgap, two important issues must be solved for successful integration of Ge into optoelectronic applications. The first is relatively high reflectance (≈30–40%) of planar surfaces of Ge that deteriorates performance of devices requiring efficient light absorption. Numerous techniques, e.g., antireflective coatings, have been proposed for enhanced light harvesting.[10] However, among those, surface nanotexturing with black Ge (b-Ge) formation is considered as one of the most promising techniques allowing effective surface reflectance suppression within the UV–visible–near-infrared (UV–vis–NIR) range for wavelengths 200–1600 nm. Here, highly efficient inductively-coupled plasma reactive ion etching provides almost 0% reflectance for Ge,[11] while metal-assisted chemical etching (MACE) allows more fast and simple route by small compromise in optical performance with reflectance below 10%.[12]

Secondly, most of the optoelectronic applications are minority carrier-based devices, which require low defect densities for good performance. While Ge bulk can easily be made of high quality by Czochralski (CZ) growth and zone refining,[13,14] the lack of stable high-quality surface passivation for a long time hampered active implementation of Ge.[15,16] Currently, two main approaches are known for managing recombination sites at the interface. First of these is called chemical passivation which assumes reducing the number of interfacial defects. In particular, germanium dioxide (GeO_2), formed by thermal oxidation of Ge, is able to provide relatively low GeO_2–Ge interface defect density securing surface recombination velocity $S_{eff} \approx 70$ cm s^{-1},[17] whereas its real application is limited by thermal instability and water-solubility as compared to analogous thermal SiO_2 for passivation of Si.[18] The second known approach relies on shielding of minority charge carriers from defects at the interface by means of internal electrical field,

M. Terletskaia, J. Isometsä, V. Vähänissi, H. Savin
Department of Electronics and Nanoengineering
Aalto University
Tietotie 3, 02150 Espoo, Finland
E-mail: mariia.terletskaia@aalto.fi

M. Miettinen, P. Laukkanen
Department of Physics and Astronomy
University of Turku
Vesilinnantie 5, 20014 Turku, Finland

The ORCID identification number(s) for the author(s) of this article can be found under https://doi.org/10.1002/pssr.202400297.

DOI: 10.1002/pssr.202400297

and so is named field-effect passivation. State-of-the-art atomic-layer-deposited (ALD) Al_2O_3 is the most common material for this type of passivation and was successfully applied for Ge surfaces reaching S_{eff} as low as 6.6 cm s^{-1}.[19,20] Significant efforts have been made to further enhance Ge surface passivation leading to such promising schemes as a-Si:H,[21] a-SiC_x/Al_2O_3,[22] a-Si:H/Al_2O_3,[23] PO_x/Al_2O_3,[24] and SiN_x/Al_2O_3.[25]

This work started when we were doing experiments on surface passivation of MACE nanotextured Ge. We made an interesting observation that the chemical solution used for MACE seemed to result in a significant reduction in S_{eff}. This unexpected outcome indicated that the MACE solution, in addition to the optics enhancement by surface nanotexturing, decreased the number of charge carrier recombination events at the interface without applying any intentional passivation. Based on the mechanism behind MACE and the highly oxidizing nature of some of the MACE solution components, we started to think that the passivation could be formed either by one of the components or by their certain mixture. Therefore, we, first, study the capability of MACE components and their mixtures to form passivation of the Ge surface. Then, we evaluate their stability and S_{eff} for the best result obtained and investigate the passivation in more detail by means of electrical, structural and chemical analysis. Finally, we compare our passivation to the state-of-the-art passivation schemes and discuss possible mechanism behind it.

2. Results

Figure 1a represents the injection-level-dependent effective minority carrier lifetimes $\tau_{eff}(\Delta n)$ measured for the samples from the first batch, which were processed in different MACE solution components and their mixtures, in comparison with as-received wafer. As can be denoted from the plot, all solutions provided passivation of Ge surface to varying degrees. Nevertheless, one can clearly distinguish three of them (DIW:HF:H_2O_2, DIW:$AgNO_3$, and DIW:H_2O_2:$AgNO_3$) leading to significantly higher lifetimes as compared to other mixtures. Moreover, a change in surface color of these samples was noticeable to the naked eye suggesting the formation of some film in each case. Among the remaining solutions with lower effective lifetimes, the original MACE (blue markers) provided slightly better passivation as compared to the others.

To obtain information about passivation quality retention in case of the three outstanding samples as well as original MACE, a stability test was done. For that $\tau_{eff}(\Delta n)$ for each sample has been measured within several days. It is important to note here that the samples were stored in nitrogen (N_2) cabinet between measurements. Each measurement was done in ambient conditions in a relatively short time (≈5 min). Obtained results (Figure 1b) showed that already the next day after processing lifetime for most of them dropped approximately by a factor of two. Meanwhile, $\tau_{eff}(\Delta n)$ for HF:H_2O_2 aqueous solution processing experienced only insignificant reduction, which suggested the stability of such Ge passivation in an inert atmosphere.

Both MACE and HF:H_2O_2 aqueous solutions led to modification of bare Ge surface by nanotexturing and film formation, respectively. In general, both of these surface modifications are likely to result in a change of surface optical properties, while the film may additionally cause parasitic light absorption by itself. These, in turn, will affect the accuracy of the lifetime measurement and subsequent S_{eff} evaluation. To eliminate the error in S_{eff}, lifetimes in the second batch of samples were measured from the unprocessed side passivated by predeposited ALD Al_2O_3 ensuring a well-defined optical constant and transparency of optical excitation during measurement. The results on $S_{eff}(\Delta n)$ evaluations for the second batch are present in **Figure 2**. According to the plot, S_{eff} for surfaces nanostructured by MACE (blue markers) and passivated by aqueous HF:H_2O_2 (red markers) was roughly the same and could be estimated to be around 14 cm s^{-1} at injection level of 1×10^{14} cm^{-3}. Following these results, passivation formed by HF:H_2O_2 aqueous solution is on par with the one provided by MACE but is far more stable. The inset in Figure 2 represents stability test that

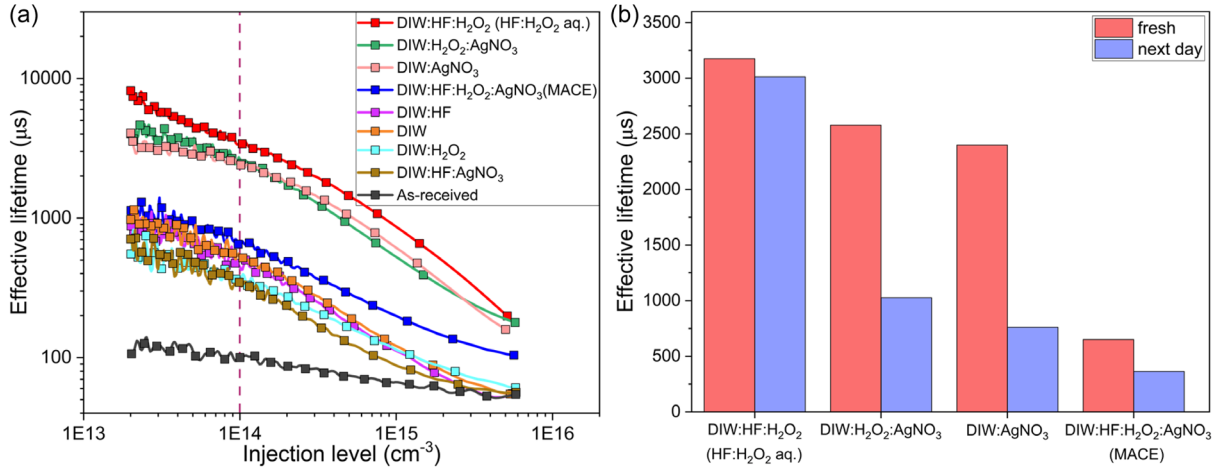

Figure 1. a) Effective lifetime (τ_{eff}) as a function of injection level for samples processed in various solutions in comparison with as-received wafer. Dashed line indicates selected injection level (1×10^{14} cm^{-3}) for lifetime comparison between the samples. b) Histogram representing change of passivation quality within 1 day after processing in the defined solutions. Effective lifetimes for comparison were extracted at the injection level of 1×10^{14} cm^{-3}.

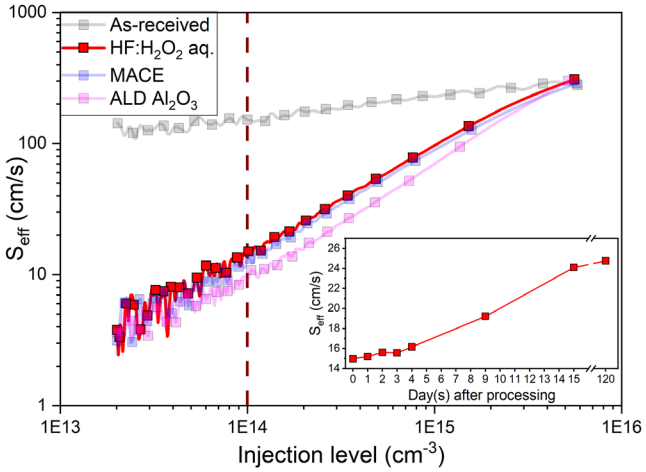

Figure 2. Surface recombination velocity (S_{eff}) as a function of minority carrier injection level for sample processed in HF:H_2O_2 aqueous solution (red markers) in comparison with MACE sample (blue markers), state-of-the-art ALD Al_2O_3 passivation of planar Ge (purple markers), and as-received unprocessed wafer (black markers). The dashed line indicates injection level used for S_{eff} extraction for comparison between the samples. The inset demonstrates results of stability test for sample processed in HF:H_2O_2 aqueous solution.

was repeated for the sample processed in HF:H_2O_2 aqueous solution. The observed slow degradation of the passivation quality within first weeks after processing was followed by stabilization with $S_{eff} \approx 24\ cm\ s^{-1}$ even after 4 months. Additionally, the initial S_{eff} gained for HF:H_2O_2 aqueous solution treatment was comparable with S_{eff} for reproduced state-of-the-art ALD Al_2O_3 passivation (purple markers, the value was introduced in experimental section as $S_{eff_{(Al_2O_3)}} \approx 9.12\ cm\ s^{-1}$).

Building on the fact that HF:H_2O_2 aqueous solution led to the formation of a specific film with promising passivating properties for Ge, further study of the film structure was carried out. First, the film was characterized by scanning electron microscopy (SEM) (**Figure 3**a) which revealed an intriguing sponge-like structure of ≈80 nm thick. The zoom-in inset allows to distinguish small particles (≈20 nm) interconnected with thin bottlenecks.

Considering the combination of highly oxidizing nature of the components of the HF:H_2O_2 aqueous solution with the generation of good passivation according to the lifetime measurements, it was supposed that the film is likely to have insulating properties. Due to our main focus on electronic properties, essential in device applications, a common starting point in evaluation of the mechanism behind the high-quality passivation is investigation of the properties at the film–bulk Ge interface. Here, standard corona oxide characterization of semiconductor (COCOS) measurement was performed for determination of thin film charge (Q_{tot}) and interface defect density (D_{it}).[26] However, the obtained results showed constant shift between contact potential difference (V_{CPD}) measurements taken under illumination and in the dark, i.e., surface band bending was unaffected by deposited corona charge (Q_c). Leakage of the Q_c was identified as the most probable cause for this phenomenon; hence, we speculated about insufficient insulating properties of the film.

To get better understanding of the mechanism behind the passivation, X-ray photoelectron spectroscopy (XPS) analysis was performed to reveal the composition of the film resulting from the treatment in HF:H_2O_2 aqueous solution. Based on the obtained spectra (Figure 3b), broadening for the bulk Ge peak can be noticed, which is most probably explained by the presence of the non-uniform porous structure previously seen in the SEM. Nevertheless, the most unexpected but important observation in Ge 3*d* region of the XPS spectra is that the film formed in the HF:H_2O_2 aqueous solution contains relatively high amount of germanium suboxides defined as GeO_x. In contrast, the sample after original MACE processing mainly had germanium dioxide (GeO_2) present.

Based on the literature survey correlated with the obtained SEM and XPS results,[27–32] we claim formation of porous

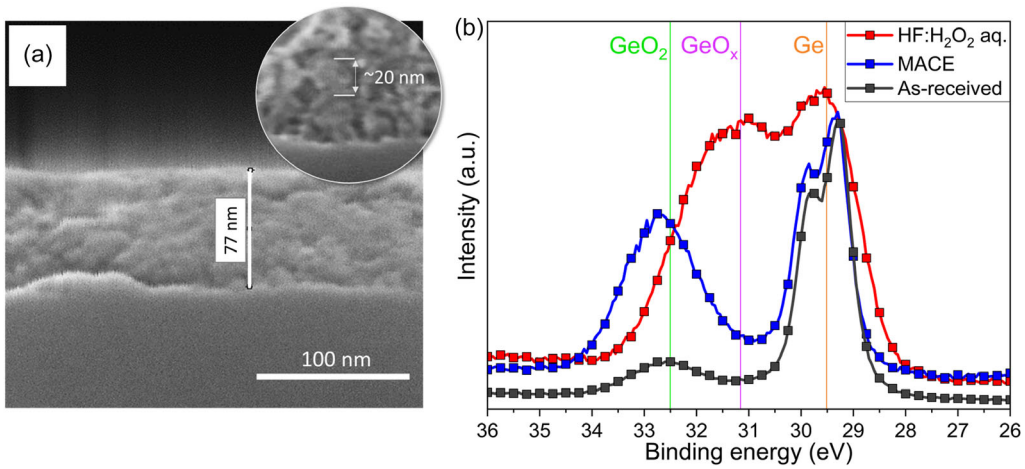

Figure 3. a) SEM image of a porous film formed on Ge surface in HF:H_2O_2 aqueous solution with estimated thickness value and inset demonstrating nanostructured nature of the film. b) Ge 3*d* region of XPS spectra measured for samples processed in MACE (blue markers) and HF:H_2O_2 aqueous (red markers) solutions in comparison with as-received unprocessed wafer (black markers). Vertical lines indicate peak position for corresponding compounds.

germanium (PGe) film with some GeO_x in it after exposing the Ge wafer to $HF:H_2O_2$ aqueous solution. Hence, the structure is highly probable to possess semiconducting properties which can fully explain the failure during COCOS measurement.

3. Discussion

The results presented in this study demonstrate that 10 min processing in the $HF:H_2O_2$ aqueous solution leads to the formation of a thin (≈80 nm) film with a sponge-like structure, which is able to provide efficient and stable surface passivation for Ge. Calculated surface recombination velocity $S_{eff} \approx 14\,cm\,s^{-1}$ secures a passivating effect almost on the level of state-of-the-art materials, e.g., ALD Al_2O_3 ($S_{eff} \approx 6.6\,cm\,s^{-1}$)[12] and PECVD a-Si:H ($S_{eff} \approx 7-17\,cm\,s^{-1}$).[21] On the other hand, the proposed chemical treatment is much faster and requires no expensive equipment or extra fabrication steps (e.g., post-deposition annealing for passivation layer activation), what endows the technology with more promise in cost-efficiency.[33] Please note that in our experiments we kept the volume of each of the original MACE solution component constant. This was an intentional choice being the most straightforward approach to pinpoint the chemical components critical for the passivation. On the other hand, this approach means that the concentrations of the components in the mixtures originating from the MACE solution vary. Now that the critical/most promising components have been identified, perhaps some further optimization could be achieved by studying the effect of their concentrations on the passivation in more detail.

To investigate the mechanism behind the passivation effect achieved by processing in $HF:H_2O_2$ aqueous solution, several characterization methods have been used. Based on the SEM and XPS results, we suggested that the film consists of PGe with some GeO_x present at least in the topmost (≤10 nm) layer. According to the XPS data, good passivation could be explained neither from chemical nor field-effect sides. First, it is known from the literature that, in general, GeO_x has no tendency to provide high-quality interface with Ge substrate compared to, for example, GeO_2 which has been observed in MACE sample.[17,34] On the other hand, XPS has analysis depth only about few nanometers and, consequently, can confirm the GeO_x presence only within the upper layer of the porous film. Therefore, these results do not rule out the possibility of existence of GeO_2 instead of GeO_x closer to the bulk Ge–porous film interface. Then, the case becomes comparable to MACE sample in terms of both lifetime and composition. Additionally, the prolonged stability of the passivation effect provided by the $HF:H_2O_2$ aqueous solution could be explained by the presence of a sponge-like structure above the interface with the bulk Ge. The porous structure may, to some extent, prevent penetration of water molecules toward the interface and, as a result, subsequent dissolution of GeO_2 there. However, an XPS depth profiling, able to provide data on the issue, would be complicated in this case. The restriction comes from the etch rate of the film that needs to be low enough to minimize damage and charging effects, making the measurement for the thickness of ≈80 nm time-consuming. And possible change in composition for shorter chemical treatments calls into question preparation of thinner films.

Meanwhile, our assumption about the film composition to be mainly PGe brings an understanding of semiconducting nature of the structure. This consideration clarifies the failure of COCOS measurement where the deposited corona charge was not able to accumulate on the surface. Moreover, the semiconducting properties lead to the fact that no fixed electrical charges, able to benefit field-effect passivation, are present within the film.

Together with the understanding of the film being a nanostructured semiconductor, another speculation on the mechanism behind the passivation effect arises. First important thing here is that Ge has a relatively large exciton Bohr radius (≈24 nm) which assures strong quantum confinement effects.[35] Based on the SEM image shown earlier, we can describe the structure as a network of relatively small (≤25 nm) Ge nanoparticles connected to each other with thin bottlenecks. Consequently, this nanosized structure has high probability of the effects dictated by quantum confinement. Based on the quantum theory, an assumption about larger bandgap of the nanostructured film in comparison with bulk Ge substrate can be made.[32] Finally, we can speculate about a situation where we have a contact between two semiconductors with different bandgaps. This contact may lead to the formation of a potential barrier at the interface which slows down or fully prevents diffusion of minority carriers toward larger bandgap material and, consequently, interfacial defect states. Additionally, the physical interface between the film and Ge substrate is probable to have a reduced number of interfacial defects. The suggestion is based on the fabrication mechanism of the porous structure which assumes etching through the Ge substrate outermost layer making the PGe film an inartificial continuation of bulk Ge substrate.

Besides the unidentified mechanism behind passivation, applicability of the technique might be currently limited or complicated in real device applications. First, the film is produced directly from the bulk Ge and, consequently, consumes the upper Ge layer. Moreover, patterning mechanisms for PGe layers are poorly investigated. On the other hand, patterning has been successfully applied for Si MACE.[36] Relying on the similarity of MACE solution compositions, applicability of the same masking techniques is expected for Ge processing. All these aspects should be considered prior integration of the technology into future device fabrication process.

4. Conclusion

This article represents efficient passivation of n-type Ge surface by wet-chemical processing in aqueous $HF:H_2O_2$ mixture, which is a derivative of the MACE solution. By the means of various characterization techniques, we demonstrated that the chemical treatment leads to the formation of thin film composed of PGe containing some GeO_x. The film ensures S_{eff} of 14 $cm\,s^{-1}$ which is comparable to values achieved by such state-of-the-art passivating materials as a-Si:H and ALD Al_2O_3. The passivation effect provided by the PGe is shown to be stable in inert N_2 atmosphere for 4 months. Unfortunately, we were unable to comprehensively determine reliably the mechanism behind Ge surface passivation provided by chemical treatment of Ge in $HF:H_2O_2$ aqueous solution. Nevertheless, several proposals regarding this issue have been made based on the data available. All in all, according to

the S_{eff} and stability evaluations, PGe can be considered a promising passivating material for Ge surfaces; however, a thorough investigation on integration of this method into device fabrication process is still required.

5. Experimental Section

The substrates used in this study were 305 µm thick n-type (antimony-doped) single-side polished CZ-grown 4″ Ge wafers with (100) orientation and 18–39 Ω cm resistivity. The original MACE process, which served as a basis for this work, was a single-step treatment in the following solution DIW:HF (50 wt%, VLSI Puranal, Honeywell):H_2O_2 (30 wt%, VLSI Puranal, Honeywell):$AgNO_3$ (0.8 wt%, ACS reagent ≥99.0%, Sigma–Aldrich) = 2156:539:11:22 mL.[12] All following chemical solutions used in this work were prepared maintaining initial volume of each component. The first batch of samples was a collection of wafer quarters processed both sides (**Figure 4**a) in various solutions according to **Table 1**.

All the treatments were performed for 10 min with periodical mixing of the solutions during processing. Finally, all samples were rinsed in deionized water (DIW) and dried with nitrogen (N_2) gas. The effect of surface passivation after each treatment was investigated based on the injection-level-dependent effective minority carrier recombination lifetime ($\tau_{eff}(\Delta n)$) measured by transient photoconductance decay technique on Sinton lifetime tester WCT-120. The measured effective lifetime was directly associated with the surface lifetime based on the equation:

$$\frac{1}{\tau_{eff}(\Delta n)} = \frac{1}{\tau_{bulk}(\Delta n)} + \frac{1}{\tau_{surface}(\Delta n)} \quad (1)$$

under assumption of high-quality substrates and, consequently, negligible bulk recombination (i.e., $\tau_{bulk}(\Delta n)$ is infinite). Additionally, $\tau_{eff}(\Delta n)$ of the so-called "as-received" wafer without any surface treatment was measured and used as a reference value within the batch. Comparison between the samples was based on the lifetimes extracted at minority carrier injection level Δn of $\approx 1 \times 10^{14}$ cm^{-3}.

The second batch relied on the results of the first batch (**Table 2**). The batch consisted of full wafers chemically processed only from the front (polished) side (Figure 4b) in HF:H_2O_2 aqueous and MACE solutions. Choice of the first solution was dictated by the results from the first batch, whereas MACE mainly served as a reference. The one-sided processing was realized by the use of a special single-wafer jig that protected the other side of the wafer from exposure to chemical solution. Prior to the chemical treatments, the rear (unpolished) surface of each wafer was coated with the ALD Al_2O_3 according to the procedure described by Isometsä et al.[20] This provided well reproducible rear surface passivation with surface recombination velocity $S_{eff_{(Al_2O_3)}} \approx 9.12$ cm s^{-1} and a known optical constant essential for more precise $\tau_{eff}(\Delta n)$ evaluation. The ALD Al_2O_3 side of the samples was illuminated for light-induced minority carrier injection in lifetime measurements. Corresponding upper limit for surface recombination velocity (S_{eff}) in each case was calculated according to

Table 1. Solution compositions used for processing of the first batch of samples.

Solution composition	Volume ratio [mL]
DIW:HF:H_2O_2:$AgNO_3$ (MACE)	2156:539:11:22
DIW	2156
DIW:HF	2156:539
DIW:H_2O_2	2156:11
DIW:$AgNO_3$	2156:22
DIW:HF:H_2O_2 (HF:H_2O_2 aq.)	2156:539:11
DIW:HF:$AgNO_3$	2156:539:22
DIW:H_2O_2:$AgNO_3$	2156:11:22

Table 2. Samples of the second batch with corresponding treatments on the front and rear sides.

Sample	Front side	Rear side
HF:H_2O_2 aqueous	DIW:HF:H_2O_2	ALD Al_2O_3
MACE[a)]	DIW:HF:H_2O_2:$AgNO_3$	ALD Al_2O_3
ALD Al_2O_3[a)]	ALD Al_2O_3	ALD Al_2O_3
As-received[a)]	–	–

[a)]Used as reference within the second batch

$$\frac{1}{\tau_{eff}(\Delta n)} \approx \frac{S_{eff}}{W} + \frac{S_{eff_{(Al_2O_3)}}}{W} \quad (2)$$

where W [cm] is the wafer thickness.[37]

The second batch included also two extra reference wafers: one was passivated by state-of-the-art ALD Al_2O_3 from both sides,[20] while another one was again "as-received" one. The latter was also used as a reference within the first batch.

Additionally, structure and composition of the film formed in HF:H_2O_2 aqueous solution were studied by SEM (FEI Helios NanoLab 600) and XPS (Thermo Scientific Nexsa G2).[38]

Acknowledgements

The authors thank the Research Council of Finland (project nos. 331313 and 338974) for financial support. The authors also thank the Finnish Ministry of Education and Culture for financial support within the pilot project MIcroELectronics doctoral school pilot (MIELi) for doctoral program (project no. VN/3137/2024-OKM-6). The work was also related

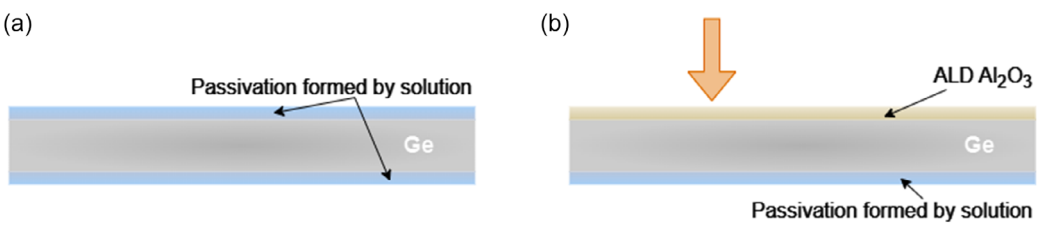

Figure 4. Schematic cross sections of chemically processed samples in the a) first and b) second batches. Orange arrow in (b) indicates the side under illumination for light-induced minority carrier injection.

to the Flagship on Photonics Research and Innovation "PREIN" funded by the Research Council of Finland, decision number 346529. The authors acknowledge the provision of facilities and technical support by the Micronova Nanofabrication Centre in Espoo, Finland, within the OtaNano research infrastructure at Aalto University.

Conflict of Interest

The authors declare no conflict of interest.

Author Contributions

Mariia Terletskaia: conceptualization (equal); investigation (equal); methodology (equal); writing—original draft; writing—review and editing (equal). **Joonas Isometsä**: conceptualization (equal); investigation (equal); writing—review and editing (equal). **Mikko Miettinen**: investigation (supporting); writing—review and editing (equal). **Pekka Laukkanen**: writing—review and editing (equal). **Ville Vähänissi**: writing—review and editing (equal). **Hele Savin**: funding acquisition (equal); supervision (equal); writing—review and editing (equal).

Data Availability Statement

The data that support the findings of this study are openly available in Zenodo at https://doi.org/10.5281/zenodo.13330359.

Keywords

germanium, porous germanium, surface passivation, wet-chemical etching

Received: September 17, 2024
Revised: November 29, 2024
Published online: February 3, 2025

[1] V. Baran, Y. Cat, T. Sertel, T. Ataser, N. A. Sonmez, M. Cakmak, S. Ozcelik, *J. Electron. Mater.* **2020**, *49*, 1249.
[2] J. van der Heide, N. E. Posthuma, G. Flamand, W. Geens, J. Poortmans, *Sol. Energy Mater. Sol. Cells* **2009**, *93*, 1810.
[3] A. Alcañiz, G. López, I. Martín, A. Jiménez, A. Datas, E. Calle, E. Ros, L. G. Gerling, C. Voz, C. del Cañizo, R. Alcubilla, *Sol. Energy* **2019**, *181*, 357.
[4] A. Ritenour, J. Hennessy, D. A. Antoniadis, *IEEE Electr. Device Lett.* **2007**, *28*, 746.
[5] D. P. Brunco, B. De Jaeger, G. Eneman, J. Mitard, G. Hellings, A. Satta, V. Terzieva, L. Souriau, F. E. Leys, G. Pourtois, M. Houssa, G. Winderickx, E. Vrancken, S. Sioncke, K. Opsomer, G. Nicholas, M. Caymax, A. Stesmans, J. Van Steenbergen, P. W. Mertens, M. Meuris, M. M. Heyns, *J. Electrochem. Soc.* **2008**, *155*, H552.
[6] K. Saraswat, C. O. Chui, T. Krishnamohan, D. Kim, A. Nayfeh, A. Pethe, *Mat. Sci. Eng. B Solid* **2006**, *135*, 242.
[7] L. Colace, G. Assanto, *IEEE Photonics J.* **2009**, *1*, 69.
[8] O. I. Dosunmu, D. D. Cannon, M. K. Emsley, B. Ghyselen, J. F. Liu, L. C. Kimerling, M. S. Ünlü, *IEEE J. Sel. Top. Quantum Electron.* **2004**, *10*, 694.
[9] P. S. Chen, S. W. Lee, M. H. Lee, C. W. Liu, *Appl. Surf. Sci.* **2008**, *254*, 6076.
[10] M. López, H. Hofer, K. D. Stock, J. C. Bermúdez, A. Schirmacher, F. Schneck, S. Kück, *Appl. Opt.* **2007**, *46*, 7337.
[11] T. P. Pasanen, J. Isometsä, M. Garin, K. X. Chen, V. Vähänissi, H. Savin, *Adv. Opt. Mater.* **2020**, *8*, 2000047.
[12] K. X. Chen, J. Isometsä, T. P. Pasanen, V. Vähänissi, H. Savin, *Nanotechnology* **2021**, *32*, 035301.
[13] S. G. Singh, D. G. Desai, A. K. Singh, S. Sen, S. C. Gadkari, S. K. Gupta, *AIP Conf. Proc.* **2012**, *1447*, 1091.
[14] G. Yang, J. Govani, H. Mei, Y. T. Guan, G. J. Wang, M. L. Huang, D. M. Mei, *Cryst. Res. Technol.* **2014**, *49*, 269.
[15] J. Oh, J. C. Campbell, *Mater. Sci. Semicond. Process.* **2010**, *13*, 185.
[16] P. W. Loscutoff, S. F. Bent, *Annu. Rev. Phys. Chem.* **2006**, *57*, 467.
[17] Y. Y. Chen, H. C. Chang, Y. H. Chi, C. H. Huang, C. W. Liu, *IEEE Electron Device Lett.* **2013**, *34*, 444.
[18] D. Kuzum, T. Krishnamohan, A. Pethe, Y. Oshima, Y. Sun, J. McVittie, P. A. Pianetta, P. C. McIntyre, K. C. Saraswat, *ECS Trans.* **2008**, *16*, 1025.
[19] W. J. H. Berghuis, J. Melskens, B. Macco, R. J. Theeuwes, M. A. Verheijen, W. M. M. Kessels, *J. Mater. Res.* **2021**, *36*, 571.
[20] J. Isometsä, T. H. Fung, T. P. Pasanen, H. C. Liu, M. Yli-koski, V. Vähänissi, H. Savin, *APL Mater.* **2021**, *9*, 111113.
[21] N. E. Posthuma, G. Flamand, W. Geens, J. Poortmans, *Sol. Energy Mater. Sol. Cells* **2005**, *88*, 37.
[22] I. Martin, G. Lopez, M. Garin, C. Vez, P. Ortega, J. Puigdollers, *Surf. Interfaces* **2022**, *31*, 102070.
[23] W. J. H. Berghuis, J. Melskens, B. Macco, R. J. Theeuwes, L. E. Black, M. A. Verheijen, W. M. M. Kessels, *J. Appl. Phys.* **2021**, *130*, 135303.
[24] R. J. Theeuwes, W. J. H. Berghuis, B. Macco, W. M. M. Kessels, *Appl. Phys. Lett.* **2023**, *123*, 091604.
[25] H. C. Liu, T. P. Pasanen, T. H. Fung, J. Isometsä, O. Leiviskä, V. Vähänissi, H. Savin, *Phys. Status Solidi A* **2023**, *220*, 2200690.
[26] M. Wilson, J. Lagowski, L. Jastrzebski, A. Savtchouk, V. Faifer, *AIP Conf. Proc.* **2001**, *550*, 220.
[27] T. Hanus, J. Arias-Zapata, B. Ilahi, P. O. Provost, J. Y. Cho, K. Dessein, A. Boucherif, *Adv. Mater. Interfaces* **2023**, *10*, 2202495.
[28] V. A. Karavanskii, A. A. Lomov, A. G. Sutyrin, V. A. Bushuev, N. N. Loikho, N. N. Melnik, T. N. Zavaritskaya, S. Bayliss, *Phys. Status Solidi A* **2003**, *197*, 144.
[29] M. Sendova-Vassileva, N. Tzenov, D. Dimovamalinovska, M. Rosenbauer, M. Stutzmann, K. V. Josepovits, *Thin Solid Films* **1995**, *255*, 282.
[30] K. Ito, D. Yamaura, T. Ogino, *Electrochim. Acta* **2016**, *214*, 354.
[31] Y. Y. Zhang, S. H. Shin, H. J. Kang, S. Jeon, S. H. Hwang, W. D. Zhou, J. H. Jeong, X. L. Li, M. Kim, *Appl. Surf. Sci.* **2021**, *546*, 149083.
[32] A. Boucherif, A. Korinek, V. Aimez, R. Arès, *AIP Adv.* **2014**, *4*, 107128.
[33] R. W. Johnson, A. Hultqvist, S. F. Bent, *Mater. Today* **2014**, *17*, 236.
[34] L. X. Zhou, J. L. Cui, X. L. Wang, S. W. Feng, *J. Mater. Sci. Mater. Electron.* **2023**, *34*, 1945.
[35] C. B. Jing, C. J. Zhang, X. D. Zang, W. Z. Zhou, W. Bai, T. Lin, J. H. Chu, *Sci. Technol. Adv. Mat.* **2009**, *10*, 065001.
[36] X. L. Liu, B. Radfar, K. X. Chen, O. E. Setala, T. P. Pasanen, M. Yli-Koski, H. Savin, V. Vähänissi, *IEEE Trans. Semicond. Manuf.* **2022**, *35*, 504.
[37] W. D. Eades, R. M. Swanson, *J. Appl. Phys.* **1985**, *58*, 4267.
[38] M. Terletskaia, J. Isometsä, M. Miettinen, P. Laukkanen, V. Vähänissi, H. Savin, *Porous Germanium for Germanium Surface Passivation*, Zenodo **2024**, https://doi.org/10.5281/zenodo.13330359.